Nonlinear adaptive depth tracking and attitude control of an underwater towed vehicle ⋆

Francisco Curado Teixeira *,⋆⋆
Antonio Pedro Aguiar⋆⋆**, Antonio Pascoal**⋆⋆

* *Centre for Environmental and Marine Studies, University of Aveiro, Portugal (e-mail: fcurado@ua.pt).*
** *Institute for Systems and Robotics and Dept. Electrical Engineering, Instituto Superior Técnico (e-mail: {pedro,antonio}@isr.ist.utl.pt)*

Abstract: This paper addresses the problem of simultaneous depth tracking and precise attitude control of an underwater towed vehicle integrated in a two-stage towing arrangement. A nonlinear Lyapunov-based output feedback controller is designed to operate in the presence of plant parameter uncertainty and proven to regulate pitch, yaw, and depth tracking errors to zero. When subjected to bounded external disturbances, the tracking errors converge to a neighborhood of the origin that can be made arbitrarily small. In the implementation proposed, a nonlinear observer is used to estimate the linear velocities used by the controller. The results obtained with computer simulations including sea wave driven disturbances and sensor noise, show that the controlled system exhibits good performance about different operating conditions and holds considerable potential for oceanographic missions that require simultaneous depth and attitude control.

Keywords: Nonlinear control; adaptive control; Lyapunov methods; trajectory tracking; underwater; towed vehicle.

1. INTRODUCTION

A great number of oceanographic missions involve data acquisition with underwater towed vehicles (towfish) that must be simultaneously controlled in depth and attitude. Missions in physical and biological oceanography often require tracking a depth profile which does not depend on the topography of the sea-floor while bottom-following is a common requirement for marine geophysical applications. In both cases, simultaneous depth and attitude control are normally required since in some of these applications the attitude of the towfish may affect significantly the quality of the data acquired. Motivated by the above problems, this paper addresses the simultaneous problem of depth and attitude control of an underwater towed vehicle.

Prior work. The problem of modeling the towing system has been addressed in prior work using either single-part towing arrangements or two-part towing systems. It has been shown that a two-stage towing arrangement can significantly attenuate towfish attitude disturbances due to the surface ship motion; see Preston (1992), Wu and Chwang (2000, 2001a,b). When modeling the motion of the gravitic depressor that induces the towfish motion we take in consideration experimental results previously obtained by other authors, either with trials at sea, cf. Preston (1989), Preston (1992), and Preston and Shupe (1993), or with scaled models in towing tanks, cf. Hopkin et al. (1993), Wu and Chwang (2001a).

Proposed approach and main contributions of this work. We tackle the problem of underwater vehicle control in the scope of nonlinear control theory. This approach was dictated mainly by the requirement that the controller should yield good performance when the vehicle undergoes motions about different equilibrium (operating) conditions and exhibit robustness against vehicle parameter uncertainty. The equilibrium conditions are determined by, among other factors, the pigtail length and the towing speed. The vehicle dynamic model adopted builds on previous work in Teixeira et al. (2006). However, in the present version we tackle the problem of controlling the vehicle's depth and attitude in both the vertical and horizontal plane, not just in the vertical plane.

2. SYSTEM CHARACTERISTICS AND MODELING

In the present study the proposed towfish specification is derived from Schuch (2004) and Schuch et al. (2005). The towing system that we consider consists of a two-part towing arrangement as illustrated in Fig. 1. The proposed vehicle is equipped with a bow plane, a stern plane, and a rudder. The sensor suite proposed includes an Attitude and Heading Unit, a depth sensor, and optionally a sonar altimeter. Justified by the requirements of some typical applications in marine geophysics and physical oceanography we require the towed vehicle to regulate the depth error to zero $\pm 0.30m$, and to regulate the pitch angle

⋆ This work was supported in part by projects GREX/CEC-IST (contract No. 035223), FREEsubNET (EU under contract number MRTN-CT-2006-036186), Co3-AUVs (EU FP7 under grant agreement No. 231378), NAV/FCT-PT (PTDC/EEA-ACR/65996/2006), and the CMU-Portugal program.
⋆⋆ The first author benefits from a postdoc fellowship of the Portuguese Foundation for Science and Technology, FCT.

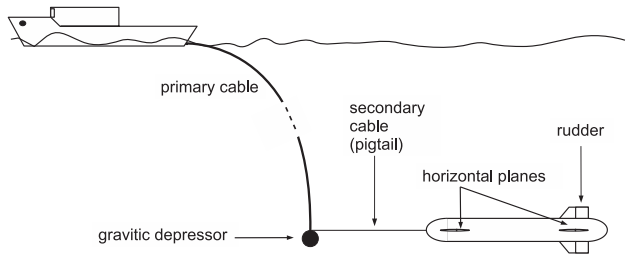

Fig. 1. Two-part towing arrangement.

and the yaw error to zero ± 1 deg; see e.g. Preston (1992), Schuch et al. (2005). The towing system and the vehicle are designed to passively stabilize the attitude in roll.

6DOF Equations of motion. In the sequel, $\{I\}$ represents an inertial coordinate frame and $\{B\}$ denotes the body-fixed frame that moves with the vehicle. The referential associated with the secondary cable is denoted $\{C\}$. Following standard notation, the vector $\eta := [x, y, z, \phi, \theta, \psi]$ represents the position and orientation of the vehicle expressed in $\{I\}$ and $\nu := [u, v, w, p, q, r]$ denotes the linear and angular components of the velocity of the vehicle expressed in $\{B\}$. When convenient, we use vectors $\eta_1 := [x, y, z]$ to represent the position of the origin of $\{B\}$ expressed in $\{I\}$ and $\eta_2 := [\phi, \theta, \psi]$ to represent the Euler angles. The velocity vector is also usually decomposed into the linear velocities represented by $\nu_1 := [u, v, w]$ and the angular velocities represented by $\nu_2 := [p, q, r]$. The towed vehicle is simulated using the three-dimensional $6DOF$ equations of motion represented in compact form by (see e.g. Fossen (2002))

$$\begin{aligned} &M\dot{\nu} + C(\nu)\nu + D(\nu)\nu + g(\eta) = \tau + \tau_e \ , \\ &\dot{\eta} = J(\eta_2)\nu, \end{aligned} \tag{1}$$

where M is the system inertia matrix, $C(\nu)$ is the Coriolis and centripetal matrix, $D(\nu)$ is hydrodynamic damping matrix, and $J(\eta)$ represents the transformation matrix from the body-fixed frame $\{B\}$ to the inertial coordinate frame $\{I\}$. The forces and moments due to actuation of the control surfaces are represented by τ. Vector τ_e includes the external forces and moments acting on the system.

Towing system and wave models. In our model of the towing system, the cable section connecting the depressor to the towfish is represented by a spring-damper system as proposed in Schuch (2004). The wave induced perturbations are modeled according to the JONSWAP wave spectrum (see e.g. Fossen (2002)) for a sea state of $3-4$. The peak frequency used in this model is a function of the modal frequency of the JONSWAP wave spectrum, the surge speed of the surface vessel, and the angle of encounter defined between the ship heading and the direction of the incident waves. The towing vessel is assumed to be operated in head seas.

3. CONTROL PROBLEM FORMULATION

3.1 Simplified equations of motion used by the controller

Kinematics. The pose of the vehicle relative to $\{I\}$ is represented by vector $X_1 := [z, \theta, \psi]'$. The velocity vector, expressed in $\{B\}$ is $X_2 := [w, q, r]'$. The simplified kinematic model based on the assumption that the vehicle is stable in *roll* is

$$\begin{aligned} \dot{z} &= -u\sin\theta + w\cos\theta, \\ \dot{\theta} &= q, \\ \dot{\psi} &= r/\cos\theta. \end{aligned} \tag{2}$$

Dynamics. Neglecting the terms due to the motion in *roll*, the relevant equations of the simplified body fixed dynamics are given by

$$\begin{aligned} &(\bar{m} - Z_{\dot{w}})\dot{w} - Z_{\dot{u}}\dot{u} - Z_{\dot{q}}\dot{q} - (\bar{m} - X_{\dot{u}})uq \\ &-Z_{|q|q}|q|q + f_w(\nu_1, \alpha, \beta) + g_w(\theta) = \\ &\bar{u}_w(\nu, \alpha, \delta) + \tau_w, \end{aligned} \tag{3}$$

$$\begin{aligned} &(I_{yy} - M_{\dot{q}})\dot{q} - M_{\dot{u}}\dot{u} - M_{\dot{w}}\dot{w} \\ &+(Z_{\dot{w}} - X_{\dot{u}})uw - I_{xz}r^2 - M_{|q|q}|q|q + f_\theta(\nu_1, \alpha, \beta) \\ &+g_\theta(\theta) = \bar{u}_\theta(\nu, \delta) + \tau_\theta, \end{aligned} \tag{4}$$

$$\begin{aligned} &(I_{zz} - N_{\dot{r}})\dot{r} - N_{\dot{v}}\dot{v} \\ &+(X_{\dot{u}} - Y_{\dot{v}})uv + I_{xz}rq - N_{|r|r}|r|r + f_\psi(\nu_1, \alpha, \beta) \\ &= \bar{u}_\psi(\nu, \beta, \delta) + \tau_\psi, \end{aligned} \tag{5}$$

where $\delta := [\delta_b, \delta_s, \delta_r]'$ is the vector of deflections of the three control surfaces, and α and β represent the angles of attack and side-slip, respectively. The variables τ_w, τ_θ, and τ_ψ denote external forces and moments resulting from the towing forces and external disturbances. The functions $\bar{u}_w(.)$, $\bar{u}_\theta(.)$, and $\bar{u}_\psi(.)$ represent the forces and moments due to the common mode $(\delta_b + \delta_s)$, differential mode $(\delta_b - \delta_s)$, and rudder (δ_r) control actions, respectively. The remaining functions, $f_w(.)$,$f_\theta(.)$, and $f_\psi(.)$ are hydrodynamic forces and moments associated with heave, *pitch* and *yaw*, respectively, and $g_w(.)$, $g_\theta(.)$, and $g_\psi(.)$ denote the restoring forces and moments. The system constants including the coefficients according to the notation of SNAME (1950) are presented in Table 1.

Linearly parameterized system. To cast the system in the form of a linear parametric model we lump all the system parameters in matrix Γ which is derived in the sequel. Define

$$a_1 := \frac{1}{\bar{m} - Z_{\dot{w}}}, \ a_2 := \frac{1}{(I_{yy} - M_{\dot{q}})}, \ a_3 := \frac{1}{(I_{zz} - N_{\dot{r}})}, \tag{6}$$

$$\begin{aligned} \Gamma_1 &:= a_1[Z_{|q|q}, (\bar{m} - X_{\dot{u}}), \bar{V}^{\frac{2}{3}}, (\bar{W} - \bar{B})]', \\ \Gamma_2 &:= a_2[M_{|q|q}, (X_{\dot{u}} - Z_{\dot{w}}), \bar{V}, \bar{B}, I_{xz}]', \\ \Gamma_3 &:= a_3[N_{|r|r}, V, -I_{xz}]', \end{aligned} \tag{7}$$

and take $A := diag(a_1, a_2, a_3) > 0$. Consider also the following functions of the measured variables:

$$\begin{aligned} \sigma_1 &:= [|q|q, uq, f_v(\nu_1)C_z(\alpha, \beta), \cos\theta]', \\ \sigma_2 &:= [|q|q, uw, f_v(\nu_1)C_M(\alpha, \beta), z_B\sin\theta, r^2]', \\ \sigma_3 &:= [|r|r, f_v(\nu_1)C_N(\alpha, \beta), rq]', \end{aligned} \tag{8}$$

with $f_v(\nu_1) := \frac{1}{2}\rho(u^2 + v^2 + w^2)$, $C_z(\alpha, \beta) := -C_{L\alpha\beta}\,\alpha$, $C_M(\alpha, \beta) := -C_{M\alpha\beta}\,\alpha$, and $C_N(\alpha, \beta) := C_{M\alpha\beta}\,\beta$.

Using the above definitions, $\Gamma := diag(\Gamma_1', \Gamma_2', \Gamma_3')$, $\Sigma := [\sigma_1', \sigma_2', \sigma_3']'$, and $f := \Gamma\Sigma$, system (3)-(5) admit the representation

$$\dot{X}_2 = f + A\bar{u} + d, \tag{9}$$

where $d := A[\tau_w, \tau_\theta, \tau_\psi]'$ represents the effect of the external forces and moments, and the control actions are represented by $\bar{u} := [\bar{u}_w, \bar{u}_\theta, \bar{u}_\psi]'$.

Table 1. Values of system parameters used in the simulations

Parameter	Symbol	Value	Units
Added mass and inertia	$X_{\dot{u}}$	-8.7849	Kg
	$X_{\dot{w}}$	0	Kg
	$Y_{\dot{v}}$	-18.64	Kg
	$X_{\dot{q}}, Y_{\dot{p}}, Y_{\dot{r}}$	0	$Kg\ m$
	$Z_{\dot{q}}$	-1.5	$Kg\ m$
	$Z_{\dot{u}}$	-1.1	Kg
	$Z_{\dot{w}}$	-18.64	Kg
	$K_{\dot{v}}$	0	$Kg\ m$
	$M_{\dot{u}}$	-2.0	$Kg\ m$
	$M_{\dot{w}}, N_{\dot{v}}$	-1.6	$Kg\ m$
	$K_{\dot{p}}, N_{\dot{p}}$	-60	$Kg\ m^2$
	$K_{\dot{r}}$	0	$Kg\ m^2$
	$M_{\dot{q}}, N_{\dot{r}}$	-260.55	$Kg\ m^2$
Moments of Inertia	I_{xx}	17.4	$Kg\ m^2$
	$I_{yy},\ I_{zz}$	174.49	$Kg\ m^2$
	I_{xz}	1.74	$Kg\ m^2$
Hydrodyn.Damping	$K_{\|p\|p}$	-125	$Kg\ m^2$
	$M_{\|q\|q}, N_{\|r\|r}$	-500	$Kg\ m^2$
	$Z_{\|q\|q}, Y_{\|r\|r}$	-10	$Kg\ m^2$
Mass of the towfish	$\bar{m}$	113.5	Kg
Towfish dry weight	$\bar{W}$	1112	N
Volume of hull	$\bar{V}$	1	m^3
Buoyancy force	$\bar{B}$	1167.6	N
Length of the body	L_b	2.75	m
C. of gravity (CG)	(x_G, y_G, z_G)	$(0, 0, 0)$	m
C. of buoyancy (CB)	(x_B, y_B, z_B)	$(0, 0, -0.08)$	m
Body lift coeff. gradient	$C_{L\alpha\beta}$	0.3508	$-$
Body pitch. coeff grad.	$C_{M\alpha\beta}$	0.1308	$-$
Gradient of fin lift coeff.	$C_{L\alpha}$	5.24	$-$
Planform area of fins	S_s	1.36	m^2
Density of water	ρ	1000	Kg/m^3

3.2 Control problem formulation

Let $z_d : [0, \infty) \to \mathbb{R}$ be a sufficiently smooth, time-varying depth reference trajectory with a uniformly bounded time-derivative, and let $X_{1d}(t) := [z_d(t), \theta_d, \psi_d]'$ represent the desired trajectory. Define also the tracking error as $\bar{e} := X_1 - X_{1d}$. The problem we address can be formally posed as follows:

Design an output feedback control law such that all closed-loop signals are bounded and the tracking error norm $\|\bar{e}\|$ converges exponentially fast to a neighborhood of the origin that can be made arbitrarily small in the presence of parameter model uncertainty.

4. OUTPUT FEEDBACK CONTROLLER DESIGN

To solve the trajectory tracking problem formulated above assuming that measurements of the linear velocities, u, v, and w are available for feedback, we propose in the sequel a Lyapunov-based adaptive control law.

4.1 Nonlinear controller design

Step1. Convergence of $\bar{e}$. Consider the Lyapunov control function $V_1 := \frac{1}{2}\bar{e}'\bar{e}$, whose time-derivative is

$$\begin{aligned}\dot{V}_1 &= (X_1 - X_{1d})'(\dot{X}_1 - \dot{X}_{1d}) \\ &= (X_1 - X_{1d})'(B^{-1}(X_2 - g) - \dot{X}_{1d}),\end{aligned} \tag{10}$$

where $B := diag(b_1, 1, 1/b_1) > 0$ and $g := [g_1, 0, 0]'$, with $b_1 := 1/\cos\theta$ and $g_1 := u\tan\theta$, assuming $|\theta| < \pi/2$. We make $\dot{V}_1$ negative definite (n.d.) using X_2 as a virtual control and setting $X_2 = B(\dot{X}_{1d} - K_a\bar{e}) + g$, for some positive definite (p.d.) diagonal matrix K_a. We require X_{1d} to be bounded and twice time-differentiable. Introducing the error variable $\bar{z} := X_2 - B(\dot{X}_{1d} - K_a\bar{e}) - g$, we rewrite (10) as

$$\dot{V}_1 = -\bar{e}'K_a\bar{e} + \bar{e}'B^{-1}\bar{z}. \tag{11}$$

Step2. Backstepping for z. For simplicity of presentation, at this stage we assume that there are no external disturbances, i.e. we use $d = 0$ in (9). This assumption will be removed later. The dynamic equation of the error $\bar{z}$ can then be written as

$$\dot{\bar{z}} = f + A\bar{u} + B(K_a\dot{\bar{e}} - \ddot{X}_{1d}) + \dot{B}(K_a\bar{e} - \dot{X}_{1d}) - \dot{g}. \tag{12}$$

We introduce the augmented Lyapunov function

$$V_2 := V_1 + \frac{1}{2}\bar{z}'\bar{z} = \frac{1}{2}\bar{e}'\bar{e} + \frac{1}{2}\bar{z}'\bar{z} \tag{13}$$

and write its time-derivative, applying (12), as

$$\begin{aligned}\dot{V}_2 = &-\bar{e}'K_a\bar{e} + \bar{z}'[B^{-1}\bar{e} + f + A\bar{u} + B(K_a\dot{\bar{e}} - \ddot{X}_{1d}) \\ &+\dot{B}(K_a\bar{e} - \dot{X}_{1d}) - \dot{g}].\end{aligned} \tag{14}$$

Our objective is to drive $\bar{z}$ to zero using the control $\bar{u}$. However, this is not practical to do because some of the parameters of the vehicle are not known with good accuracy. Hence, we define the variables $\hat{a}_1$, $\hat{a}_2$, $\hat{a}_3$, $\hat{\Gamma}_1$, $\hat{\Gamma}_2$, and $\hat{\Gamma}_3$ to represent estimates of a_1, a_2, a_3, Γ_1, Γ_2, and Γ_3 respectively, and set the control using the estimated model parameters as follows:

$$\begin{aligned}\bar{u} := -\hat{A}^{-1}[&B^{-1}\bar{e} + \hat{f} + B(K_a\dot{\bar{e}} - \ddot{X}_{1d}) \\ &+\dot{B}(K_a\bar{e} - \dot{X}_{1d}) - \dot{g} + K_b\bar{z}],\end{aligned} \tag{15}$$

where K_b is a p.d. diagonal matrix, $\hat{A} := diag(\hat{a}_1, \hat{a}_2, \hat{a}_3)$, and $\hat{f} := \hat{\Gamma}\Sigma = diag(\hat{\Gamma}_1', \hat{\Gamma}_2', \hat{\Gamma}_3')\Sigma$.

Define $\Pi := [\Gamma, A]'$ and the estimation errors $\tilde{A} := A - \hat{A}$, $\tilde{\Gamma} := \Gamma - \hat{\Gamma}$, and $\tilde{\Pi} := \Pi - \hat{\Pi}$ with $\hat{\Pi} := [\hat{\Gamma}, \hat{A}]'$, and take $\Phi := [\Sigma', -(\hat{A}^{-1}(\hat{\Gamma}\Sigma + B^{-1}\bar{e} + B(K_a\dot{\bar{e}} - \ddot{X}_{1d}) + \dot{B}(K_a\bar{e} - \dot{X}_{1d}) - \dot{g} + K_b\bar{z}))']'$. Using the control law (15), straightforward algebraic manipulations yield the time-derivative of V_2 as

$$\begin{aligned}\dot{V}_2 &= -\bar{e}'K_a\bar{e} - \bar{z}'K_b\bar{z} + \bar{z}'[\tilde{\Gamma}\Sigma - \hat{A}^{-1}\tilde{A}(\hat{\Gamma}\Sigma + B^{-1}\bar{e} \\ &\quad +B(K_a\dot{\bar{e}} - \ddot{X}_{1d}) + \dot{B}(K_a\bar{e} - \dot{X}_{1d}) - \dot{g} + K_b\bar{z})] \\ &= -\bar{e}'K_a\bar{e} - \bar{z}'K_b\bar{z} + \bar{z}'\tilde{\Pi}'\Phi.\end{aligned} \tag{16}$$

Step3. Adaptive control. At this stage we introduce a third Lyapunov function that captures the effect of the error in the estimation of the system's parameters:

$$V_3 := V_2 + \frac{1}{2k_1}\left\|\tilde{\Pi}\right\|_F^2 = \frac{1}{2}\bar{e}'\bar{e} + \frac{1}{2}\bar{z}'\bar{z} + \frac{1}{2k_1}\left\|\tilde{\Pi}\right\|_F^2 \tag{17}$$

for some scalar $k_1 > 0$, where $\|.\|_F$ stands for the Frobenius norm. The time-derivative of V_3 is

$$\dot{V}_3 = -\bar{e}'K_a\bar{e} - \bar{z}'K_b\bar{z} + \mathbf{tr}(\tilde{\Pi}'(\Phi\bar{z}' - \frac{1}{k_1}\dot{\hat{\Pi}})). \tag{18}$$

Let $\hat{\Pi}_0$ represent an initial estimate of Π and take $\tilde{\Pi}_0$ as an upper bound on the error $\Pi - \hat{\Pi}_0$. Setting de dynamics of $\hat{\Pi}$ as

$$\dot{\hat{\Pi}} = k_1[\Phi\bar{z}' - k_2(\hat{\Pi} - \hat{\Pi}_0)] \tag{19}$$

for some scalar $k_2 > 0$ yields

$$\dot{V}_3 = -\bar{e}' K_a \bar{e} - \bar{z}' K_b \bar{z} + \mathbf{tr}(k_2 \tilde{\Pi}' (\hat{\Pi} - \hat{\Pi}_0)).$$

The effect of the scalar gain k_2 in the adaptive control law (19) is to ensure that the values of the system parameters estimated by the adaptive controller remain inside a ball with the center defined by the initial estimate $\hat{\Pi}_0$. Applying the equality $\mathbf{tr}(k_2 \tilde{\Pi}' (\hat{\Pi} - \hat{\Pi}_0)) = -\frac{1}{2} k_2 \left\| \tilde{\Pi} \right\|_F^2 - \frac{1}{2} k_2 \left\| \hat{\Pi} - \hat{\Pi}_0 \right\|_F^2 + \frac{1}{2} k_2 \left\| \Pi - \hat{\Pi}_0 \right\|_F^2$ it follows that

$$\dot{V}_3 \leq -\bar{e}' K_a \bar{e} - \bar{z}' K_b \bar{z} - \frac{1}{2} k_2 \left\| \tilde{\Pi} \right\|_F^2 + \frac{1}{2} k_2 \left\| \tilde{\Pi}_0 \right\|_F^2. \quad (20)$$

Although we cannot ensure that $\dot{V}_3$ is always negative, we show in the sequel that this is sufficient to ensure practical stability (Jiang et al. (1994)).

External forces. At this stage we remove the simplifying assumption made in *Step 2*, and consider the external forces and moments represented by d in (9). Noting that these are unknown terms that cannot be taken into account in the control law (15) we obtain, instead of (16),

$$\dot{V}_2 = -\bar{e}' K_a \bar{e} - \bar{z}' K_b \bar{z} + \bar{z}' \tilde{\Pi}' \Phi + \bar{z}' d, \quad (21)$$

and

$$\dot{V}_3 \leq -\bar{e}' K_a \bar{e} - \bar{z}' K_b \bar{z} - \frac{1}{2} k_2 \left\| \tilde{\Pi} \right\|_F^2 + \frac{1}{2} k_2 \left\| \tilde{\Pi}_0 \right\|_F^2 + \bar{z}' d. \quad (22)$$

4.2 Stability analysis

Theorem I Consider the closed-loop system $\mathbf{\Sigma}$ consisting of the vehicle model (2)-(5) and the adaptive feedback controller (12), (15), and (19). Given a bounded, sufficiently smooth time-varying reference trajectory $X_{1d} : [0, \infty) \rightarrow \mathbb{R} \times (-\frac{\pi}{2}, \frac{\pi}{2}) \times [-\pi, \pi]$, the following holds:

i) For any initial condition, the solution to $\mathbf{\Sigma}$ exists globally, all closed-loop signals are bounded, and the tracking error $\bar{e}$ satisfies

$$\|\bar{e}\| \leq \mathbf{e}^{-\lambda t} c_0 + \epsilon, \quad (23)$$

where λ, c_0, and ϵ are positive constants, and c_0 depends on the initial conditions.

ii) By appropriate choice of the parameter K_b, the rate of convergence λ and the radius ϵ can be chosen at will.

Proof Starting with (22) we apply Young's inequality to show that for any scalar constant $\kappa > 0$

$$\dot{V}_3 \leq -\bar{e}' K_a \bar{e} - \bar{z}' (K_b - \frac{\kappa}{2} I) \bar{z} - \frac{1}{2} k_2 \left\| \tilde{\Pi} \right\|_F^2 + \frac{1}{2} \Delta^2, \quad (24)$$

where $\Delta = \frac{d_b}{\sqrt{\kappa}} + \sqrt{k_2} \left\| \tilde{\Pi}_0 \right\|_F$ with $d_b := \sup_{t \geq 0} \|d\|$. From (17) and (24), and assuming that K_b satisfies $K_b > \frac{\kappa}{2} I$ we conclude that there is a constant λ that verifies simultaneously $0 < \lambda \leq k_1 k_2, \lambda I \leq K_a, and \lambda \leq 2K_b - \kappa I$, such that the following inequality holds:

$$\dot{V}_3 \leq -\lambda V_3 + \frac{1}{2} \Delta^2. \quad (25)$$

We prove (i) by applying the Comparison Lemma (Khalil (2002)) and showing that along the solutions of $\mathbf{\Sigma}$

$$V_3(t) \leq \mathbf{e}^{-\lambda t} V_3(0) + \frac{1}{2\lambda} \Delta^2. \quad (26)$$

This shows that all the control signals remain bounded and the solutions of the system exist globally and are ultimately bounded with ultimate bound $\frac{1}{2\lambda} \Delta^2$. Considering the definition of V_3, we conclude from (26) that $\|\bar{e}\|$ converges to a ball of radius $\frac{\Delta}{\sqrt{2\lambda}}$. We can also conclude that the closed-loop system is input-to-state practically stable (ISpS) with respect to bounded parametric uncertainties and bounded external disturbances.

To prove (ii) we show that it is possible to make the radius $\frac{\Delta}{\sqrt{2\lambda}}$ arbitrarily small by an appropriate choice of the controller parameters. For a given limiting radius ϵ and a given convergence rate λ we have

$$\frac{\Delta}{\sqrt{2\lambda}} \leq \epsilon = \frac{d_b}{\sqrt{2\lambda\kappa}} + \sqrt{\frac{k_2}{2\lambda}} \left\| \tilde{\Pi}_0 \right\|_F.$$

Thus, we can select

$$\kappa := d_b^2 / 2\lambda \left(\epsilon - \sqrt{\frac{k_2}{2\lambda}} \left\| \tilde{\Pi}_0 \right\|_F \right)^2$$

provided that we make

$$K_b - \frac{\kappa}{2} I = K_b - \frac{d_b^2}{2\lambda \left(\epsilon - \sqrt{\frac{k_2}{2\lambda}} \left\| \tilde{\Pi}_0 \right\|_F \right)^2} I \geq \frac{\lambda}{2} I > 0.$$

Thus, it is shown that (25) is verified and therefore (26) holds.

4.3 Coupling the horizontal and vertical planes

When considering the effects of motion in *roll*, the following coupling terms must be inserted in the dynamic equations of the system:

$$\Gamma_{c1} := a_1[-(\bar{m} - Y_{\dot{v}}), (\bar{W} - \bar{B})]',$$
$$\Gamma_{c2} := a_2[(I_{zz} - I_{xx} + K_{\dot{p}} - N_{\dot{r}}), -I_{xz}]',$$
$$\Gamma_{c3} := a_3[(I_{xx} - I_{yy} + M_{\dot{q}} - K_{\dot{p}}), I_{xz}]',$$
$$\sigma_{c1} := [vp, \cos\theta(cos\phi - 1)]',$$
$$\sigma_{c2} := [pr, p^2]', \quad \sigma_{c3} := [pq, p^2]'.$$

The system dynamics can be reformulated by substituting the new expressions for Γ, Σ, B, and g as follows. Make

$$\Gamma := diag([\Gamma_1', \Gamma_{c1}'], [\Gamma_2', \Gamma_{c2}'], [\Gamma_3', \Gamma_{c3}']),$$
$$\Sigma := [\sigma_1', \sigma_{c1}', \sigma_2', \sigma_{c2}', \sigma_3', \sigma_{c3}']',$$
$$B := diag(b_1 + b_{c1}, 1 + b_{c2}, 1/b_1 + b_{c3}),$$
$$g := [g_1 + g_{c1}, g_{c2}, g_{c3}]',$$

with b_1 and g_1 defined in Section 4.1, $b_{c1} := (1 - \cos\phi)/\cos\theta\cos\phi$, $b_{c2} := (\cos\phi - 1)/\cos\phi$, $b_{c3} := \cos\theta(1 - 1/\cos\theta)$, $g_{c1} := u\tan\theta(1/\cos\theta - 1) - v\tan\phi$, $g_{c2} := r\tan\phi$, and $g_{c3} := -q\tan\phi$. Let the coupling components of the system dynamics be represented by

$$\Omega_c := [\Gamma_{c1}' \sigma_{c1} + g_{c1}, \Gamma_{c2}' \sigma_{c2} + g_{c2}, \Gamma_{c3}' \sigma_{c3} + g_{c3}]',$$

and let b_u,b_v, and b_p denote the upper bounds on the surge and sway velocities, and roll rate, respectively. Simple algebraic manipulations show that

$$\|\Omega_c\|^2 \leq C_c \|X_2\|^2 + \Delta_c, \quad (27)$$

where C_c and Δ_c are constants. Applying a reasoning similar to the one used in Theorem I it can be concluded that

$$V_3(t) \leq \mathbf{e}^{-\lambda t} V_3(0) + \gamma_c(\|X_2\|) + \frac{\nabla}{\lambda}, \tag{28}$$

where the class K function γ_c and the positive constant $\frac{\nabla}{\lambda}$ represent the coupling terms not compensated by the control $\bar{u}$. Hence, we conclude that the system is ISpS with respect to bounded unmodeled dynamics.

5. NONLINEAR OBSERVER DESIGN

To simplify the proposed implementation we assume now that no direct measurements of surge, sway, and heave are available for feedback. It is assumed that the surge velocity is constant, i.e. $u = u_0$. The heave velocity component is estimated by a nonlinear observer that is described in the sequel. Consider the state space representation

$$\begin{aligned} H\dot{x}_o &= F_\theta x_o + f_o(\theta, q, \tau_w) + g_o(x_o, \delta), \\ y_o &= z, \end{aligned} \tag{29}$$

where $x_o := [z, w]'$, $H := diag(1, M_{3,3})$, $F_\theta := \begin{bmatrix} 0 & \cos\theta \\ 0 & C_v \end{bmatrix}$, $f_o(\theta, q, \tau_w) :=$

$$\begin{bmatrix} -u_0 \sin\theta \\ (\bar{m} - X_{\dot{u}})u_0 q + Z_{|q|q}|q|q + (\bar{W} - \bar{B})\cos\theta + \tau_w \end{bmatrix},$$

and $g_o(x_o, \delta) := [0, -\frac{1}{2}\rho S_s C_{L\alpha}(u_0^2 + w^2)\delta_c]'$, with $\delta_c := \delta_b + \delta_s$, $M_{3,3} := \bar{m} - Z_{\dot{w}} > 0$, and $Cv := -\frac{1}{2}\rho(\bar{V}^{\frac{2}{3}} C_{L\alpha\beta} + 2S_s C_{L\alpha})(u_0 + 0.3) < 0$. Let $\hat{w}$ represent the estimated value of w and define $\tilde{w} := w - \hat{w}$. Here we use the approximation $f_v(\nu_1)C_z(\alpha, \beta) \approx -\frac{1}{2}\rho C_{L\alpha\beta}(u_0 + 0.3)w$. Using the expression for the dynamics of w derived from (3) we implement an observer of this variable as follows:

$$\begin{aligned} H\dot{\hat{x}}_o &= F_\theta \hat{x}_o + f_o(\theta, q, \tau_w) + g_o(\hat{x}_o, \delta) + K_o(y_o - \hat{y}_o), \\ \hat{y}_o &= h'\hat{x}_o, \end{aligned} \tag{30}$$

where $h := [1, 0]'$ and $K_o := [\kappa_1, \kappa_2]'$ is the gain of the observer, with κ_1 and κ_2 defined in the sequel.

Using $\tilde{x}_o := x_o - \hat{x}_0$, $\delta_o := -\frac{1}{2}\rho S_s C_{L\alpha}\delta_c$, and $\tau_o := g_o(x_o, \delta) - g_o(\hat{x}_o, \delta) = [0, \delta_o(w^2 - \hat{w}^2)]'$ the observer error dynamics becomes

$$H\dot{\tilde{x}}_o = F_\theta \tilde{x}_o - K_o h'\tilde{x}_o + \tau_o. \tag{31}$$

We introduce the Lyapunov function $V_o := \tilde{x}_o' H \tilde{x}_o$ whose time derivative is

$$\dot{V}_o = -\tilde{x}_o' A_o \tilde{x}_o + 2\tilde{x}_o'\tau_o, \tag{32}$$

with $A_o := (K_o h' + hK_o' - F_\theta - F_\theta') > 0$ for $\kappa_1 > 0, \kappa_2 \geq 1$.

Given an upper bound b_w on w, it is straightforward to show that

$$\begin{aligned} \dot{V}_o &= -\tilde{x}_o' A_o \tilde{x}_o + 2\delta_o \tilde{w}^2(w + \hat{w}) \\ &\leq -\tilde{x}_o' \left[A_o - 2\left|\delta_o(b_w + \hat{w})\right| I\right] \tilde{x}_o \end{aligned}. \tag{33}$$

To make $A_o - 2\left|\delta_o(b_w + \hat{w})\right| I > 0$ the following condition must hold:

$$\left|\delta_o(b_w + \hat{w})\right| < \left|C_v\right|. \tag{34}$$

Condition (34) establishes the region of attraction of the origin of $\tilde{x}_o$ which depends on the towing velocity. Thus, although it is not possible to ensure global stability, through proper manipulation of the observer gains κ_1 and κ_2 the initial condition of $\tilde{x}_o$ can be made arbitrarily large, that is, we have semi-global asymptotic stability.

Stability of controller-observer system. We assume that measurements of the variable z are affected by noise n_z with bounded intensity. Using the stability properties of the controller and the observer, application of the Small-Gain Theorem (Jiang et al. (1994)) shows that the interconnected controller-observer system is ISpS.

6. RESULTS OF SIMULATIONS AND DISCUSSION

In this section we illustrate the performance of the control algorithms developed through computer simulations.

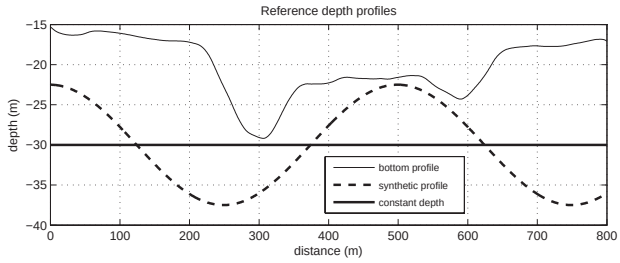

Fig. 2. Reference depth profiles used in simulations. Depths are represented by negative values to facilitate the visualization of the depth profile.

In the scenario used for simulations the towed vehicle is required to regulate the pitch angle and the yaw error to zero while tracking a desired depth profile with total length of approximately 800m. Three types of depth trajectories were used as shown in Fig. 2: a real bathymetric profile, a sinusoidal reference, and a constant depth trajectory. We simulated the system with nominal towing speeds equal to 3knts, 4knts, 6knts, and 8knts, using pigtail lengths of 30m, 50m, and 100m.

Systems's parameters and constraints. The initial estimates of the model parameters represented by Π_0 are set to $\pm 10\%$ of the corresponding true values. The control planes have a maximum deflection of ± 20 deg and the actuators' dynamics are approximated by a first order system with a time constant equal to 0.1s.

Measurement noise. To test the robustness of the proposed adaptive controller with respect to sensor noise, the simulated measurements of z, θ, ψ, q, and r are affected by additive gaussian white noise with standard deviations $\sigma_z = 0.1m$, $\sigma_\theta = 0.1\,\text{deg}$, $\sigma_\psi = 1\,\text{deg}$, and $\sigma_q = \sigma_r = 0.5\,\text{deg}/s$, respectively.

6.1 Results and discussion

In Fig. 3 the performance of the non-controlled system is compared with that of the controlled system subjected to the same wave-driven disturbances.

System performance in constant-depth tracking and bottom following. The results of simulations show that the motion of the controlled vehicle is in accordance with our

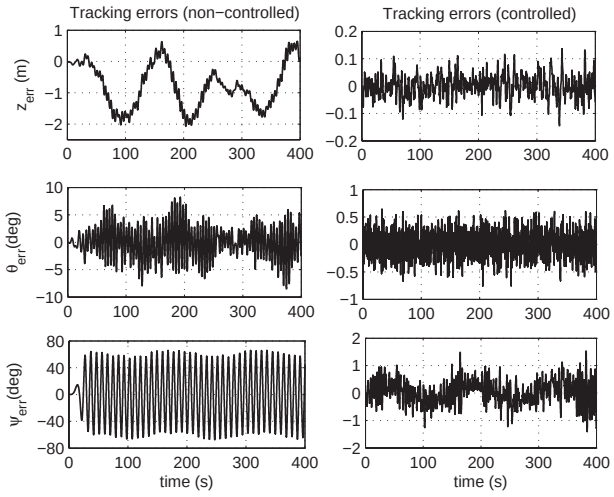

Fig. 3. Tracking errors obtained by the non-controlled system (left) and the controlled system (rigth). Constant depth tracking at 4knts towing speed.

previous assumption of negligible motion in roll. The angle of roll verifies $|\phi| < 0.25°$ in all the simulated scenarios. The estimation error achieved by the observer of w is very small ($|w| < 0.05m/s$) and decreases significantly with increasing towing speeds as expected from the theoretical results of stability analysis. Noting that bottom following is the most demanding scenario in terms of control, we observe that at $4knts$ towing speed, depth and *pitch* errors verify $|\bar{e}_z| \leq 0.3m$ and $|\bar{e}_\theta| < 1\,\text{deg}$, respectively; see Fig.4. The 2σ interval of the yaw error corresponds to $|\bar{e}_\psi| < 0.9\,\text{deg}$.

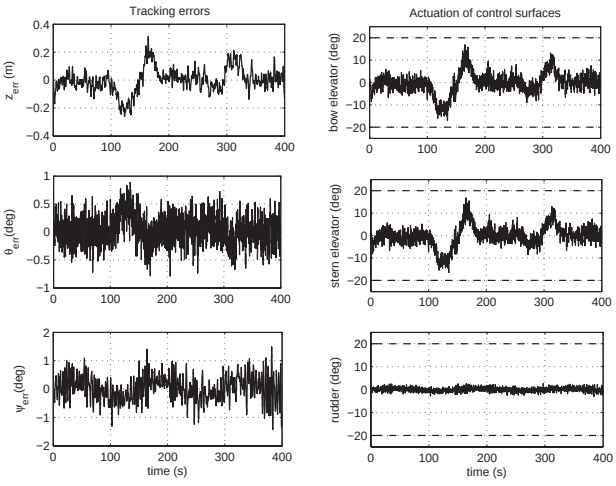

Fig. 4. Tracking errors and actuation of the control surfaces in a simulated bottom-following mission at 4knts towing speed. The upper and lower dashed lines in the actuation plots represent the hard-limits of deflection of the control planes.

Impact of pigtail length and towing speed on system performance. The results of the tests show that the impact of the length of the secondary cable in the tracking errors obtained by the controlled system is not significant. However, there is a significant impact in surge speed and lateral motion of the towfish. As such, to mitigate accelerations in surge or lateral oscillations of the towfish position a longer pigtail is recommended. The impact of different towing speeds on the performance of the controlled system is very small for towing speeds smaller than 6knts. Even at this speed the tracking errors remain inside the limits specified for the system.

7. CONCLUSIONS AND FUTURE WORK

The paper addressed the problem of controlling an underwater towed vehicle in the vertical and horizontal planes. The system analyzed consisted a two-stage towing arrangement which includes a long primary cable, a gravitic depressor, and a secondary cable. Although the paper did not address modeling the primary cable, the simulations used realistic wave models to derive the motion of the depressor-pigtail subsystem which transmits the wave driven disturbances to the towfish. We conclude that, with an appropriate choice of the pigtail length and towing speed, the tracking errors achieved by the controlled system comply with the specifications imposed by the applications that motivated the system design. For applications that require a precise control of lateral position we propose a fully actuated system equipped with two vertical control surfaces. This will be the subject of future research.

REFERENCES

Fossen, T. I., 2002. Marine Control Systems. Guidance, Navigation, and Control of Ships, Rigs and Underwater Vehicles. Marine Cybernetics.

Hopkin, D., Preston, J. M., Latchman, S., 1993. Effectiveness of a two-part tow for decoupling ship motions. In: OCEANS'93 IEEE Conference. Vol. I. Victoria, Canada, pp. 359–364.

Jiang, Z. P., Teel, A. R., Praly, L., 1994. Small-gain theorem for ISS systems and applications. Mathematics of Control, Signals, and Systems (7), pp. 95–120.

Khalil, H. K., 2002. Nonlinear Systems, 3rd Edition. Prentice Hall.

Preston, J. M., 1992. Stability of towfish used as sonar platforms. In: OCEANS '92 IEEE Conference. Vol. 2. Newport, Rhode Island, USA, pp. 888 – 893.

Preston, J. M., Shupe, L., 1993. Remote mine-hunting systems - vehicle stability trials. Tech. Rep. RMC-PROC-93-P-115, Defence Research Establishment Pacific, Victoria BC (CAN).

Preston, J. M., 1989. Stability of towfish as sonar platforms and benefits of the two-part tow. Technical Memorandum 89-19. Research and Development Branch - Department of National Defence - Canada.

Schuch, E. M., 2004. Towfish design, simulation and control. MSc thesis. Virginia State University - Aerospace Engineering Dept.

Schuch, E. M., Linklater, A. C., Lambeth, N. W., Woolsey, C. A., 2005. Design and simulation of a two stage towing system. In: OCEANS 2005 MTS/IEEE Conference. Washington, D. C., USA.

SNAME, 1950. The society of naval architects and marine engineers. Nomenclature for treating the motion of a submerged body through a fluid. Technical and Research Bulletin 1 (57).

Teixeira, F. C., Aguiar, A. P., Pascoal, A., 2006. Nonlinear control of an underwater towed vehicle. In: MCMC'2006 - 7th IFAC Conference on Manoeuvring and Control of Marine Craft. Lisbon, Portugal.

Wu, J., Chwang, A. T., 2000. A hydrodynamic model of a two-part underwater towed system. Ocean Engineering 27 (5), 455–472.

Wu, J., Chwang, A. T., 2001a. Experimental investigation on a two-part underwater towed system. Ocean Engineering 28 (6), 735–750.

Wu, J., Chwang, A. T., 2001b. Investigation on a two-part underwater manoeuvrable towed system. Ocean Engineering 28 (8), 1079–1096.